LBL-35841
UC-405

Lawrence Berkeley Laboratory
UNIVERSITY OF CALIFORNIA

Engineering Division

Presented at the International Symposium on Optics, Imaging Instrumentation, San Diego, CA, July 25–26, 1994, and to be published in the Proceedings

Ghost Images and Feasibility of Reconstructions with the Richardson-Lucy Algorithm

J. Llacer and J. Nuñez

July 1994

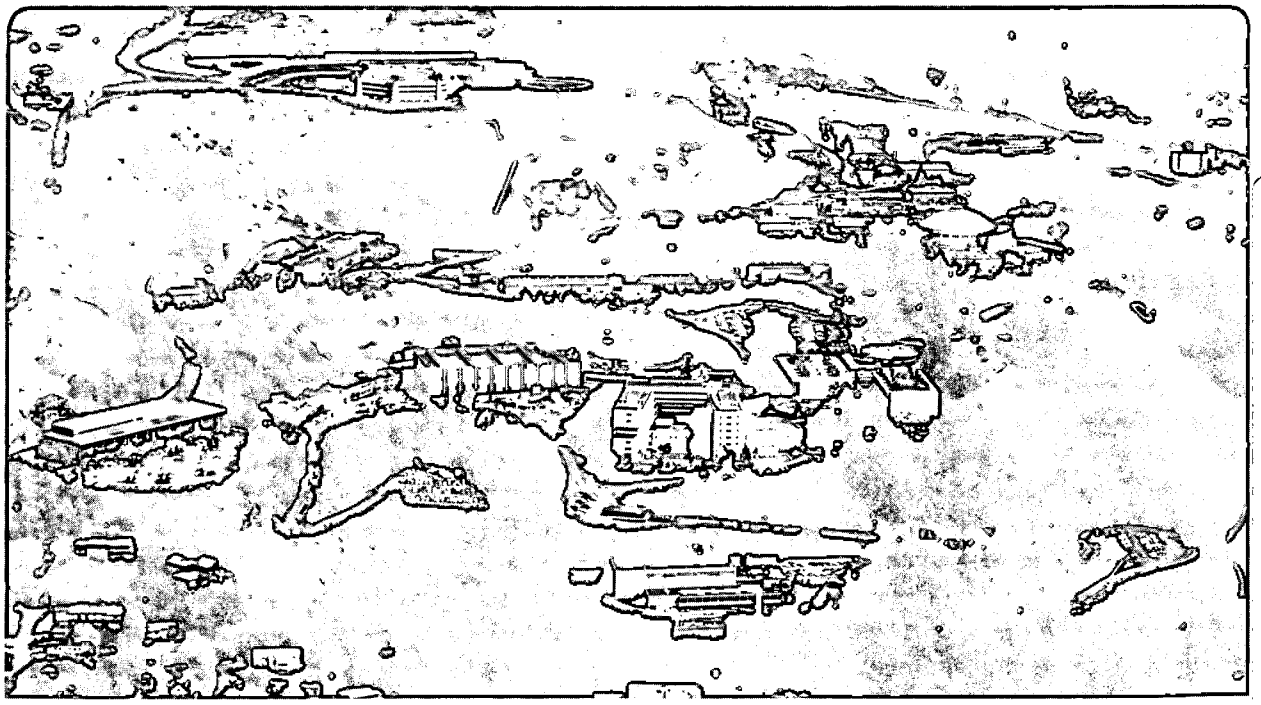

REFERENCE COPY
Does Not
Circulate
Bldg. 50 Library.
LBL-35841
Copy 1

Prepared for the U.S. Department of Energy under Contract Number DE-AC03-76SF00098

DISCLAIMER

This document was prepared as an account of work sponsored by the United States Government. While this document is believed to contain correct information, neither the United States Government nor any agency thereof, nor the Regents of the University of California, nor any of their employees, makes any warranty, express or implied, or assumes any legal responsibility for the accuracy, completeness, or usefulness of any information, apparatus, product, or process disclosed, or represents that its use would not infringe privately owned rights. Reference herein to any specific commercial product, process, or service by its trade name, trademark, manufacturer, or otherwise, does not necessarily constitute or imply its endorsement, recommendation, or favoring by the United States Government or any agency thereof, or the Regents of the University of California. The views and opinions of authors expressed herein do not necessarily state or reflect those of the United States Government or any agency thereof or the Regents of the University of California.

LBL-35841
UC-405

GHOST IMAGES AND FEASIBILITY OF RECONSTRUCTIONS WITH THE RICHARDSON-LUCY ALGORITHM

Jorge Llacer
Engineering Division
Lawrence Berkeley Laboratory
University of California, Berkeley, California 94720

and

Jorge Nuñez

Departament d'Astronomia i Meteorologia
Universitat de Barcelona and Observatorio Frabra
Barcelona, Spain

July 1994

The work was supported by the Director, Office of Energy Research,
Office of Health and Environmental Research, Physical and Technological Division,
of the U.S. Department of Energy under Contract No. DE-AC03-76SF00098.
Jorge Nunez has been supported by, in part, by the DGICYT
Ministerio de Educacion y Ciencia (Spain)
under Grant No. BP90-0478 and fellowship No. BEC 91-328.
Partial support for the collaborative work has been obtained
from the Generalitat de Catalunya and the Gaspar de Portola Catalonian Studies
Program of the University of California, Berkeley.

LBL-35841
UC-405

GHOST IMAGES AND FEASIBILITY OF RECONSTRUCTIONS WITH THE RICHARDSON-LUCY ALGORITHM

Jorge Llacer

Engineering Division
Lawrence Berkeley Laboratory
University of California, Berkeley, California 94720

and

Jorge Nuñez

Departament d'Astronomia i Meteorologia
Universitat de Barcelona and Observatorio Frabra
Barcelona, Spain

ABSTRACT

This paper is the result of a question that was raised at the recent workshop on "The Restoration of HST Images and Spectra II", that took place at the Space Telescope Science Institute in November 1993, for which there was no forthcoming answer at that time. The question was: What is the null space (ghost images) of the Richardson-Lucy (RL) algorithm?. Another question that came up for which there is a straight-forward answer was: What does the MLE algorithm really do?. In this paper we attempt to answer both questions.

This paper will begin with a brief description of the null space of an imaging system, with particular emphasis on the Hubble telescope. The imaging conditions under which there is a possibly damaging null space will be described in terms of linear methods of reconstruction. For the uncorrected Hubble telescope, it is shown that for a PSF computed by TINYTIM on a 512 x 512 dimension, there is no null space. We introduce the concept of a "nearly null" space, with an unsharp distinction between the "measurement" and the "null" components of an image and generate a reduced resolution Hubble Point Spread Function (PSF) that has that nearly null space. We then study the propagation characteristics of null images in the Maximum Likelihood Estimator (MLE), or Richardson-Lucy algorithm, and the nature of its possible effects, but we find in computer simulations that the algorithm is very robust to those effects: if they exist,the effects are local and tend to disappear with increasing iteration numbers. We then demonstrate how a PSF that has small components in frequency domain results in noise magnification, just as one would expect in linear reconstruction. The answer to the second question is given in terms of the residuals of a reconstruction and the concept of feasibility.

1. INTRODUCTION

In the workshop on "The Restoration of HST Images and Spectra II" that took place at the Space Telescope Science Institute in November 1993, a question was raised as to what is the null space (ghost images) of the Richardson-Lucy algorithm. This question has been studied thoroughly in the medical tomography image reconstruction community for some period of time, since there are instruments that do suffer strongly from null space effects, with consequent problems when linear methods of reconstruction are attempted. The Maximum Likelihood Estimator (MLE), or Richardson-Lucy algorithm, can handle the null space effects readily without any catastrophic artifacts in the reconstructions and the expectation in our mind was that the same would be true in reconstructions for the Hubble telescope. In this paper, we examine the concept of "measurement" and "null" components of images and their relationship to linear and MLE methods of reconstruction. In particular we show that the Point Spread Function (PSF) of the uncorrected Hubble telescope does not lead to a null component. We then generate the PSF of a hypothetical lower resolution Hubble telescope that can lead to "near null" components and show the theoretical propagation

characteristics of those components in the MLE algorithm. Reconstruction experiments are then described that show the "benign" behavior of the algorithm with respect to "near null" components, except in the presence of noise, in which case there is a typical trade-off between resolution and noise. We finally discuss what the MLE algorithm really does in terms of the residuals of the reconstruction and the relationship between the residuals and feasibility.

2. GHOST IMAGES

2.1 Linear methods

2.1.1 Image reconstruction

We consider the imaging equation

$$\mathbf{g} = \mathbf{H}\mathbf{f} \tag{1}$$

where $\mathbf{g}$ and $\mathbf{f}$ are stacked image vectors of length n^2, for an n x n image plane, and $\mathbf{H}$ is an $n^2 \times n^2$ matrix that contains in each row (or column) the stacked form of the space invariant point response function (PRF) of the system being considered. We make the implicit assumption that $\mathbf{g}$ and $\mathbf{f}$ are replicated in the (x,y) plane and that the rows (or columns) of $\mathbf{H}$ are rotated complete versions of the same function, so that Fourier transform methods can be applied.

The singular value decomposition (SVD) of a general square matrix results in the representation[1]

$$\mathbf{H} = \mathbf{U}\Lambda\mathbf{V}^t \tag{2}$$

where $\mathbf{U}$ is a matrix with columns containing the left eigenvectors of $\mathbf{H}$, $\mathbf{V}$ contains the right eigenvectors and Λ is a diagonal matrix of eigenvalues, all of dimensions $n^2 \times n^2$. Some of the elements of Λ may be zero, indicating that $\mathbf{H}$ is not of full rank R.

For the conditions indicated above, $\mathbf{H}$ is block circulant and the $\mathbf{U}$ and $\mathbf{V}$ matrices become $\mathbf{F}$, a stacked version of a 2-d Fourier transform matrix. Then, the imaging equation (1) becomes[2]

$$\mathbf{g} = (\mathbf{F}\Lambda\mathbf{F})\mathbf{f} \tag{3}$$

and, since $\mathbf{F}$ is unitary, the estimate $\hat{\mathbf{f}}$ can be obtained from

$$\hat{\mathbf{f}} = \left(\mathbf{F}\Lambda^{-1}\mathbf{F}\right)\mathbf{g}, \tag{4}$$

where Λ^{-1} is diagonal with entries given by the reciprocal of the eigenvalues contained in Λ.

This is the familiar linear method of reconstruction. The elements of Λ^{-1} corresponding to zero eigenvalues are set to zero before the reconstruction and some filtering of the remaining diagonal entries of Λ^{-1} can be carried out in order to reduce noise in the estimation.

The eigenvalues contained in Λ correspond to an ordered version of the results of obtaining a Fourier transform of the point spread function (PSF) of the imaging system. In the case of a useful telescope, if we assume that sources in the sky $\mathbf{f}$ are band-limited and properly sampled, and we use that same sampling to describe the PSF, it appears unlikely that there will be any elements of Λ that are identically zero, i.e., the matrix $\mathbf{H}$ will be of full rank. There can be, however, many elements that are relatively small, corresponding to a small response of the telescope to the corresponding frequencies. These are the elements that would be filtered out in linear reconstruction to avoid excessive noise.

2.1.2 Ghost images

A ghost image or null component $\mathbf{f}_{null}$ of an image is the information in an image that does not appear in the data[1], i.e.,

$$\mathbf{H}\mathbf{f}_{null} = 0. \tag{5}$$

With respect to the imaging equation (3), we can separate $\mathbf{f}$ into the measurement component $\mathbf{f}_{meas}$ and the null component,

$$\mathbf{g} = (\mathbf{F}\Lambda\mathbf{F})(\mathbf{f}_{meas} + \mathbf{f}_{null}) \tag{6}$$

and, evidently, for $\mathbf{f}_{null}$ to have no effect on $\mathbf{g}$, it is necessary that the frequency components of $\mathbf{f}_{null}$ correspond to eigenvectors on Λ that are exactly zero, or perhaps very small to have any significant effect on the mesured data $\mathbf{g}$.

In the context of a telescope, given a particular set of sources of photons in the sky, $\mathbf{f}$, the corresponding $\mathbf{f}_{null}$ is interesting because that part of the image will not be represented in the data and one should not attempt to recover it in the reconstruction process. It is interesting to note that for $\mathbf{H}$ having only positive entries, $\mathbf{f}_{null}$ has to have positive and negative values if (5) is to hold, except in the trivial case of $\mathbf{f}_{null} = 0$.

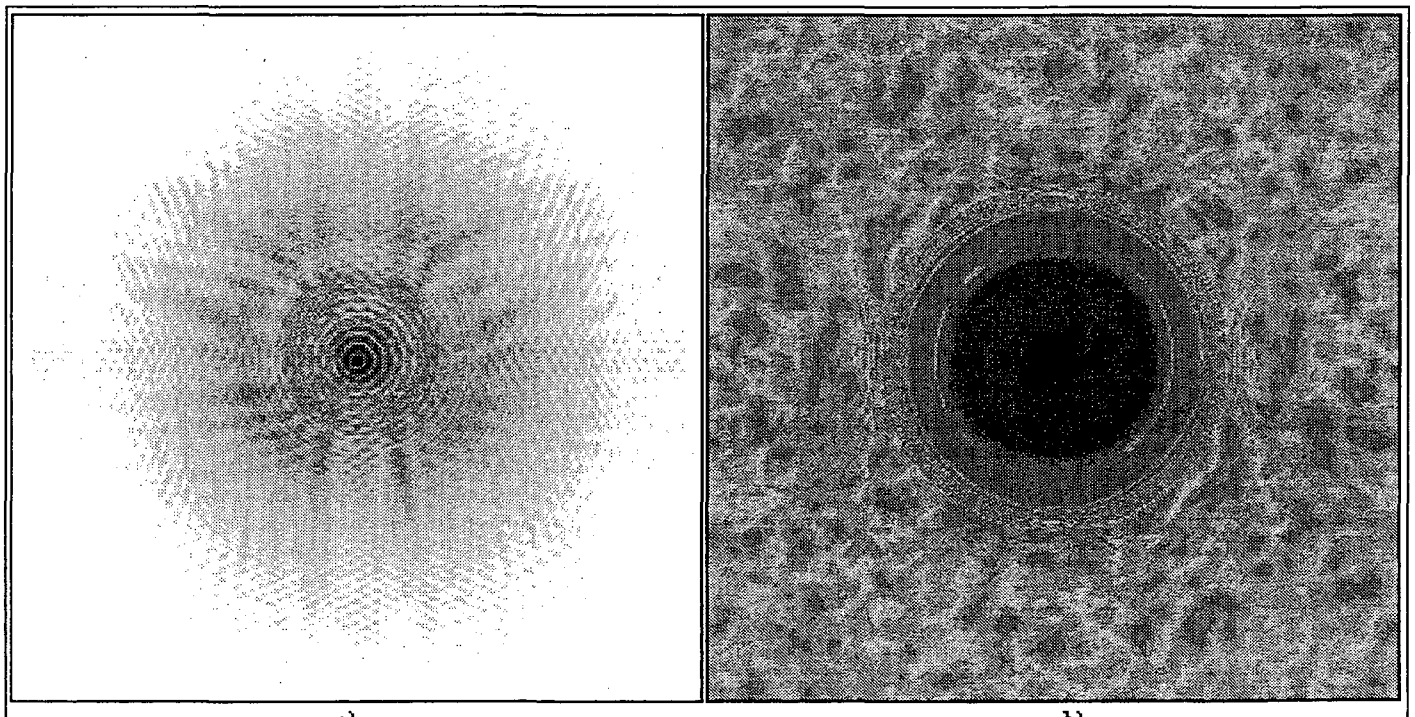

a) b)

Fig. 1 - PSF of the uncorrected Hubble telescope. Logarithmic gray scales. a) Calculated by TINYTIM, subsampled by a factor of 3. b) Magnitude of the Fourier transform.

2.1.3 Example based on the uncorrected Hubble telescope

Figure 1a) shows the PSF of the uncorrected Hubble telescope subsampled by a factor of 3, computed by TINYTIM, in a logarithmic gray scale, with dimension 512 x 512 pixels. Figure 1b) shows the magnitude of the Fourier transform of the PSF, also in a logarithmic scale. An examination of the characteristics of the Fourier transform of the PSF carried out by filtering out its higher frequency "skirts" indicates that the information carried by those higher frequencies is a necessary part of the PSF, i.e.,

the "skirts" of the transform can neither be considered zero nor too small. We conclude, therefore, that the PSF of Fig. 1 does not lead to null images. We can artificially create an example of a PSF that should have null images for practical purposes: We consider a hypothetical telescope that, in addition to the aberrations of the uncorrected Hubble telescope, exhibits a Gaussian blurring function with a certain standard deviation σ. Figure 2a) shows the new PSF for a value of σ = 1.7 pixels (FWHM = 4.0 pixels) and Fig. 2b) shows the magnitude of its Fourier transform. Figs. 1b) and 2b) are normalized to a maximum of 1.0 at zero frequency. The same gray levels have been used in both cases, with values below 10^{-7} shown as white. Fig. 3 shows cuts through the central axis of the Fourier transforms of both the Hubble PSF and the new PSF, which we will call "reduced resolution" telescope PSF, in a log10 scale. It should be mentioned at this point that the assumption indicated above that $\mathbf{f}$ is band-limited and properly sampled is quite important. If the assumption does not hold, there will be a null space corresponding to all the high frequencies that are not represented in the sampling, although the above formalism does not describe that case.

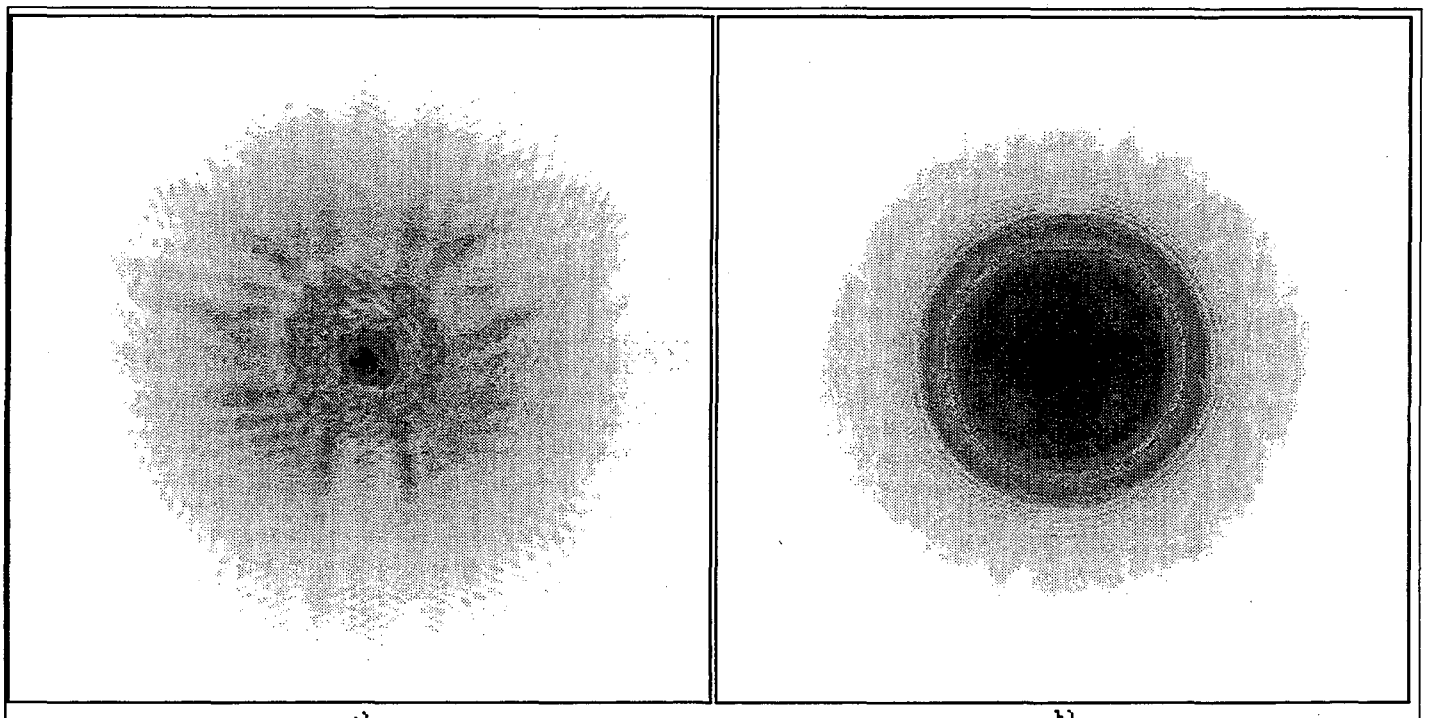

a) b)

Fig. 2 - PSF of reduced resolution Hubble telescope. Logarithmic gray scales. a) PSF calculated by convolution of the PSF of Fig. 1a) with a Gaussian of σ = 1.7 pixels. b) Corresponding magnitude of the Fourier transform, shown with the same color scale as Fig. 1b).

The PSF of the reduced resolution telescope has Fourier coefficients at the higher frequencies which are many orders of magnitude smaller than the corresponding ones of the normal telescope. One would expect that the measurement component $\mathbf{f}_{meas}$ for the reduced resolution case could be obtained by Fourier transforming a given distribution $\mathbf{f}$, removing the Fourier components that correspond to the small values in the PSF and inverse transforming. This is, however, not a good procedure in our case. Any attempt at filtering with a low pass filter of sharp cutoff a distribution $\mathbf{f}$ that has features with large differences in intensity and high frequencies will lead to objectionable "ringing" in $\mathbf{f}_{meas}$. Shepp-Logan, Butterworth and other filters used in medical tomography could be used for the purpose, with substantially reduced ringing, but they will always introduce some information into $\mathbf{f}_{meas}$ that was not in $\mathbf{f}$. The only linear filter that is assured not to introduce new information is a Gaussian. If we use such a filter, we establish an "unsharp" distinction between $\mathbf{f}_{meas}$ and $\mathbf{f}_{null}$: ghost images, if they exist, will be represented in the data with higher intensity if they contain lower frequencies. It appears that this unsharp distinction is the only practical way of defining ghost images in a general astronomical case.

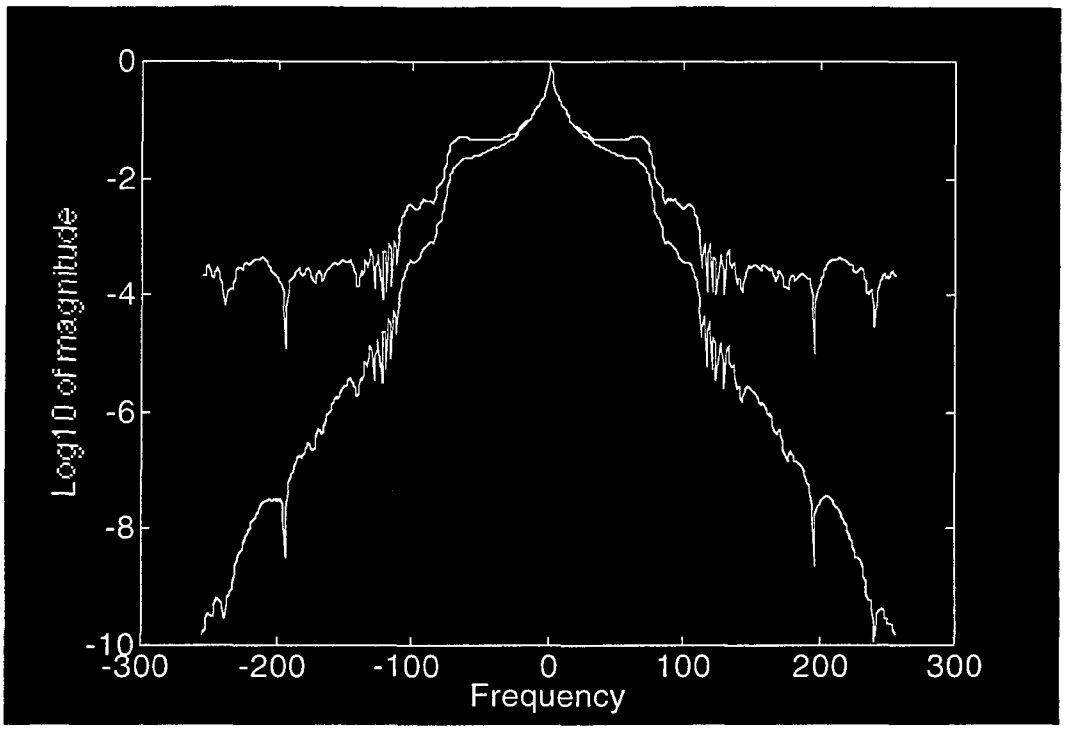

Fig. 3 - Cut through the center line of Fourier transform of PSF's. Shown are values for the uncorrected Hubble telescope and for the hypothetical "reduced resolution" Hubble telescope.

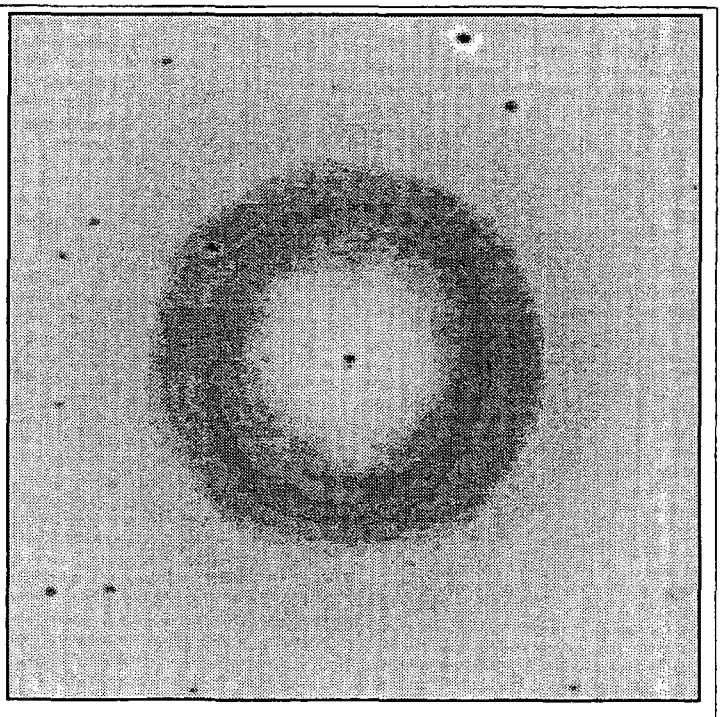

Fig. 4 - Phantom "pn" used for the tests reported in this paper. Log scale, generated by STSCI for reconstruction tests.

In order to investigate the above concepts in practice, we start by assuming that the radiation field $\mathbf{f}$ in the sky is given by Fig. 4. This is a noise-free phantom generated at STSCI for the study of reconstruction algorithms. It contains stars of substantially different intensity levels, and a "nebula" with some structures of various intensities, including one star. The original phantom was of dimension 256 x 256. All images will be shown in that same dimension, altough all the computational work has been done at 512 x 512, with appropriate zero padding. It should be noted that the Fourier transform of $\mathbf{f}$ has significant values up to the limit of the sampling frequency.

Fig. 5a) shows $\mathbf{f}_{meas}$ obtained by masking off the high frequencies of the Fourier transform of $\mathbf{f}$ outside of a circle of radius 170 pixels in frequency domain, corresponding to frequencies in the reduced resolution PSF with response 7 orders of magnitude below that of the zero frequency. The "ringing" effect indicated above is quite evident. Fig. 5b) shows $\mathbf{f}_{meas}$ for the case in which the Gaussian with σ = 1.7 pixels has been used as a filter. The interpretation of Fig. 5b) is that, in the process of removing the Hubble aberrations by reconstruction of the reduced resolution data,

we should only attempt to obtain the resolution shown in the figure if ghost image effects in the reconstruction are to be kept at a minimum. Attempts at recovering some of the resolution lost by the reduced resolution telescope may result in possibly objectionable ghost effects, although we have not yet described what those effects could be.

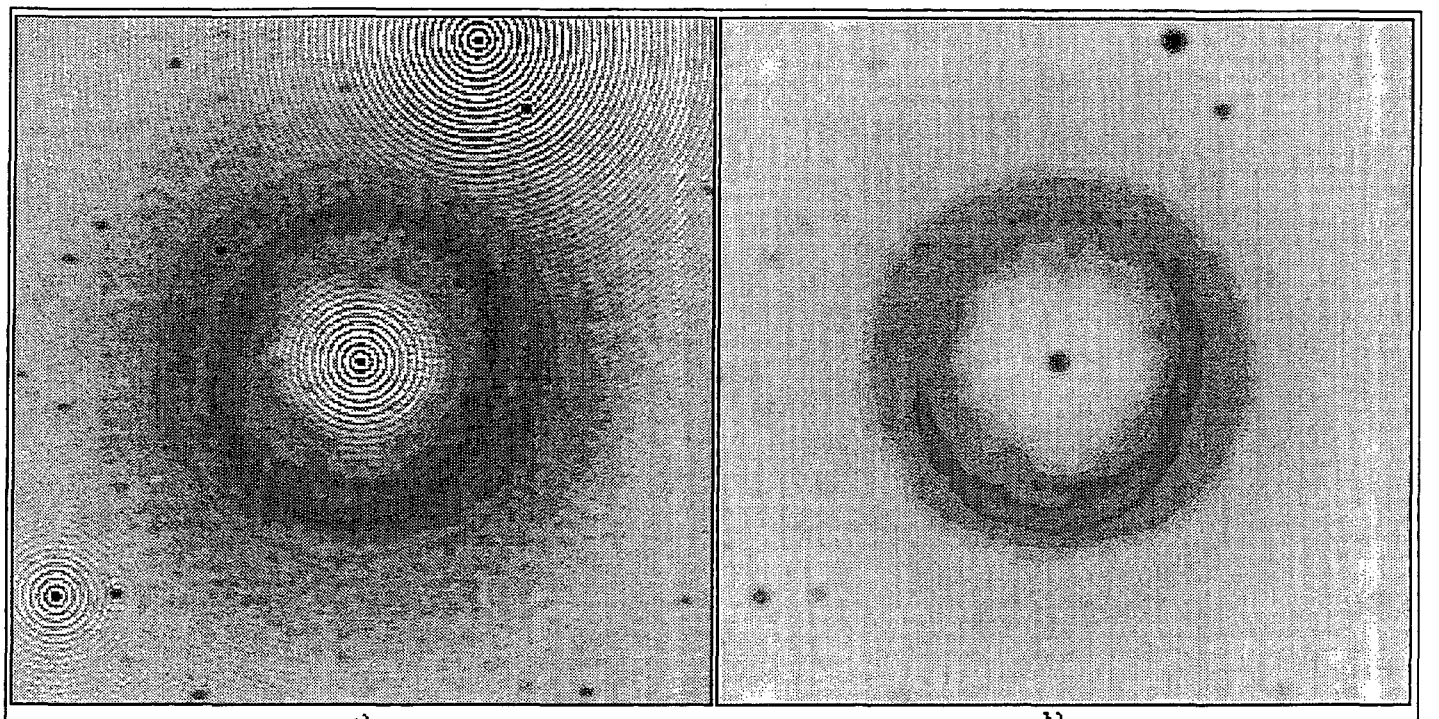

a) b)

Fig. 5 - Measurement components of the phantom of Fig. 4 for the PSF of the "reduced resolution" telescope. a) Obtained by masking off high frequencies with a sharp cutoff. b) By filtering with the Gaussian kernel that resulted in reduced resolution.

2.2 Maximum Likelihood Estimator (MLE) methods

2.2.1 Theoretical analysis

We consider the case of a simple Maximum Likelihood Estimator (MLE)[3] or the Richardson-Lucy algorithm[4,5] for the case with individual photons being counted, without corrections or other factors that can disturb the Poisson nature of the detection process. We assume that the PSF of the system can lead to null images and we want to investigate their propagation during the MLE iterative process.

We will use the following notation:

f_i - the intensity value of the i th pixel in the true radiation source in the sky, stacked notation.

$\hat{f}_i^{(k)}$ - the value of the i th pixel in the estimate of that radiation source, at iteration (k).

$\hat{f}_{\mathrm{m}i}^{(k)}$ - the value of the i th pixel in the measurement part of the estimate.

$\hat{f}_{\mathrm{n}i}^{(k)}$ - the value of the i th pixel in the null part of the estimate

g_j - the value of the j th pixel in the measured data.

h_{ji} - the probability that a photon emitted at f_i is detected at g_j. We consider the columns of $\mathbf{H}$ to be properly normalized to unity.

Let's assume that at some iteration k we have an estimate of the radiation source in the sky which we can consider free from ghost image effects, with pixel values $\hat{f}_i^{(k)}$. At that point, a ghost image $\hat{f}_{\mathrm{n}i}$ is introduced into the reconstruction process by addition to the current estimate. After iteration $(k+1)$, the result will contain two parts:

$$\hat{f}_{\mathrm{m}i}^{(k+1)} + \hat{f}_{\mathrm{n}i}^{(k+1)} = \left(\hat{f}_i^{(k)} + \hat{f}_{\mathrm{n}i}\right)\sum_j \frac{g_j h_{ji}}{\sum_l h_{jl}\left(\hat{f}_l^{(k)} + \hat{f}_{\mathrm{n}l}\right)} \tag{7}$$

Since by definition of a null image $\sum_l h_{jl}\hat{f}_{\mathrm{n}l} = 0$, the measurement part of the $(k+1)$ iteration will still be free from influence by the ghost image, i.e., $\hat{f}_{\mathrm{m}i}^{(k+1)} = \hat{f}_{\mathrm{m}i}$. However, the null part of the $(k+1)$ iteration will have evolved with the same corrections as the measurement part.

Let's now go one step further into the $(k+2)$ iteration. The results will be

$$\hat{f}_{\mathrm{m}i}^{(k+2)} + \hat{f}_{\mathrm{n}i}^{(k+2)} = \left(\hat{f}_i^{(k+1)} + \hat{f}_{\mathrm{n}i}^{(k+1)}\right)\sum_j \frac{g_j h_{ji}}{\sum_l h_{jl}\left(\hat{f}_l^{(k+1)} + \hat{f}_{\mathrm{n}l}^{(k+1)}\right)} \tag{8}$$

In this case, we cannot expect that $\sum_l h_{jl}\hat{f}_{\mathrm{n}l}^{(k+1)}$ will be zero in the denominator of (8) and, therefore, the effect of the ghost image will be felt in both the measurement and the null images of the results and will propagate thereafter.

The question then arises of how a null image can be introduced into the iterative process, or rather, whether it is possible to carry out a reconstruction without introducing a null image. It would appear that, no matter what initial image is used as $f_i^{(0)}$, it can always be considered to consists of two parts

$$f_i^{(0)} = f_{\mathrm{m}i}^{(0)} + f_{\mathrm{n}i}^{(0)} \tag{9}$$

although the null portion is not explicitly known. As a result, the effect of ghost images could appear in MLE reconstructions, unless filtered out at each iteration. We will next test whether effects due to propagation of ghost images are of significance with the MLE.

2.2.2 Propagation tests

Let's consider the uncorrected Hubble and the reduced resolution telescopes described in Section 2.1.3. We will assume that we have a radiation field $\mathbf{f}$ in the sky given by Fig. 4 and we will compare the performance of the MLE for noise-free data obtained from both telescopes in two cases: a) starting with a uniform image field and b) starting with a field that contains null components.

2.2.2.1 Data Generation

We have started by taking the radiation field $\mathbf{f}$ and convolving it with the Hubble and the reduced response PSF's, yielding noise-free data for both telescopes. For case a), the initial image $f_i^{(0)}$ has been a 512 x 512 uniform field with a total number of counts equal to the number of counts in the data file. For case b), ghost images have been introduced into the

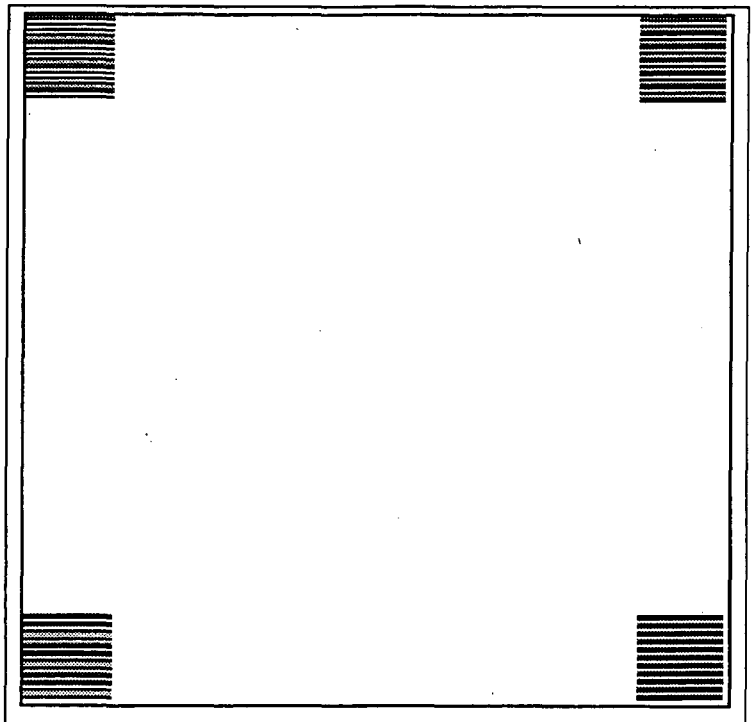

Fig. 6 - Initial image containing sinusoidally spaced bars for tests of propagation of null components. The background is a uniform field with 8.55 counts per pixel.

reconstruction by using an initial image $f_i^{(0)}$ containing four subsections with sinusoidal bars in one direction. The bars appear at frequencies between 7/8 to 3/4 of the sampling frequency. The rest of the field was uniform, with a total number of counts again equal to the number of counts in the data file, although this is not at all critical . Fig. 6 shows the $f_i^{(0)}$ used for the experiments with ghost images.

2.2.2.2 Results of reconstructions

a) Uniform initial field.

The purpose of noise-free reconstructions with a uniform initial field has been to find out whether ghost images would appear spontaneously in a reconstruction when the PSF was such that it had a number of very small Fourier components, as is the case with the reduced resolution case under study. For noise-free data, the MLE procedure should yield images that are arbitrarily close to the original image $\mathbf{f}$ as the iterative procedure progresses. We have chosen the reconstruction results at iteration 1000 for the Hubble telescope simulation as results without ghost image effects. Figure 7a) shows those reconstruction results. Table I shows a comparison of enclosed energy in a 3 x 3 pixel array centered on stars of different intensities for the original true image $\mathbf{f}$ and for the reconstructions discussed in this section. The 3 x 3 pixel array may be too small to adequately describe the photometric behavior of the algorithm and the data in Table I should be taken only as a sensitive indication of convergence towards the original image $\mathbf{f}$. It is evident that 1000 iterations was not quite enough to recover full resolution in the weaker stars, but the results will be considered acceptable for our current purpose. No acceleration methods have been used in the algorithm and all the reconstructions have been carried out in single precision arithmetic. Fig. 7b) shows the results of using the reduced resolution data and PSF. In order to obtain similar resolution as with the case of Fig. 7a) we have had to carry out 4000 iterations. Energy enclosed results for this case are also shown in Table I. The two images in Fig. 7 are essentially identical, with only minor differences in the "halos" around the bright stars. It appears, therefore, that the MLE algorithm is robust against PSF's that have very small frequency components, at least for noise-free data.

TABLE I

Energy included in 3 x 3 pixel area, for different reconstructions. Noise-free case.
Data do not represent photometric behavior, but indicate resolution achieved.

Star description	True data	Hubble, 1000 its.	Red. res., 4000 its.
Brightest star	51457	51167	50054
Central star	15125	14206	13390
Star included in nebula	5127	3997	3793
Low intensity star	1077	871	764

b) Initial field with added null components.

Reconstructions with null components introduced into the initial image field, in the "unsharp" distinction case discussed in Section 2.1.3, should converge to results that respond only to the data, since the MLE is known to converge to a single

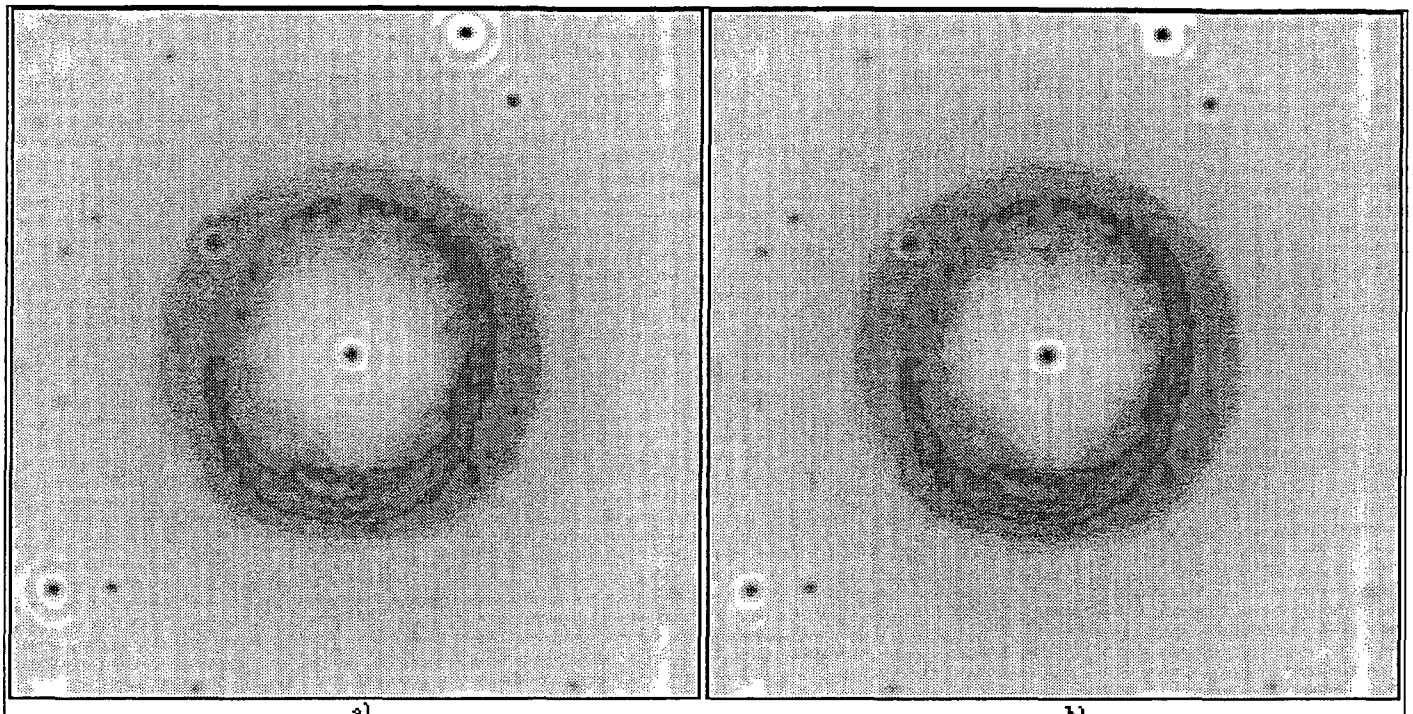

a) b)

Fig. 7 - Results of reconstructing noise-free simulation data to check for a possible spontaneous generation of null component effects. a) Hubble simulation and corresponding PSF, 1000 its. b) Reduced resolution simulation and PSF, 4000 its.

maximum, although it could be a rather broad one. One would expect, therefore, that the bars added to the initial image will disappear at high iterations numbers, at least with "good" PSF's. The purpose of the reconstruction experiments reported in this section has been to see whether noise-free images obtained from the reduced resolution data and PSF would show the bar patterns more prominently than in the Hubble simulation case, for the same resolution in stars, when the reconstruction process is stopped relatively early. Fig. 8a) shows the result of reconstructing the Hubble telescope simulation to iteration 500 and Fig. 8b) shows the results for the reduced resolution telescope at iteration 2000. Table II shows the energy enclosed in the same 3 x 3 pixel array as in Table I for both reconstructions, with the addition of the measured standard deviations in 7 x 7 pixel arrays centered in the 4 bar zones at the periphery of the images. The latter are a measure of the contrast of the sinusoidal bars. The two reconstructions have approximately the same resolution at the stars and approximately the same contrast in the bar patterns, with no other effects due to the introduced ghost images. The effects predicted by the analysis of Section 2.2.1 turn out to be "local", i.e., they do not propagate from their original pixel locations and tend to disappear when iterating towards convergence. The algorithm shows "forgiving" characteristics, for noise-free data.

2.2.3 Reconstructions with Poisson noise

The reconstructions with noise-free data have provided a degree of confidence about the behavior of the MLE algorithm when using PSF's that have Fourier components with small magnitudes: no unexpected objects will appear in images due to systematic characteristics of the algorithm. With Poisson noise, however, we can expect that the characteristics of the PSF will have a strong effect on the quality of the images that can be recovered.

2.2.3.1 Data generation and reconstruction

The data used in Section 2.2.2 have been modified by calculating Poisson instances of the mean values represented by the noise-free data. The procedure "poidev.c" described in "Numerical Recipes in C" has been used for that purpose[6]. The number

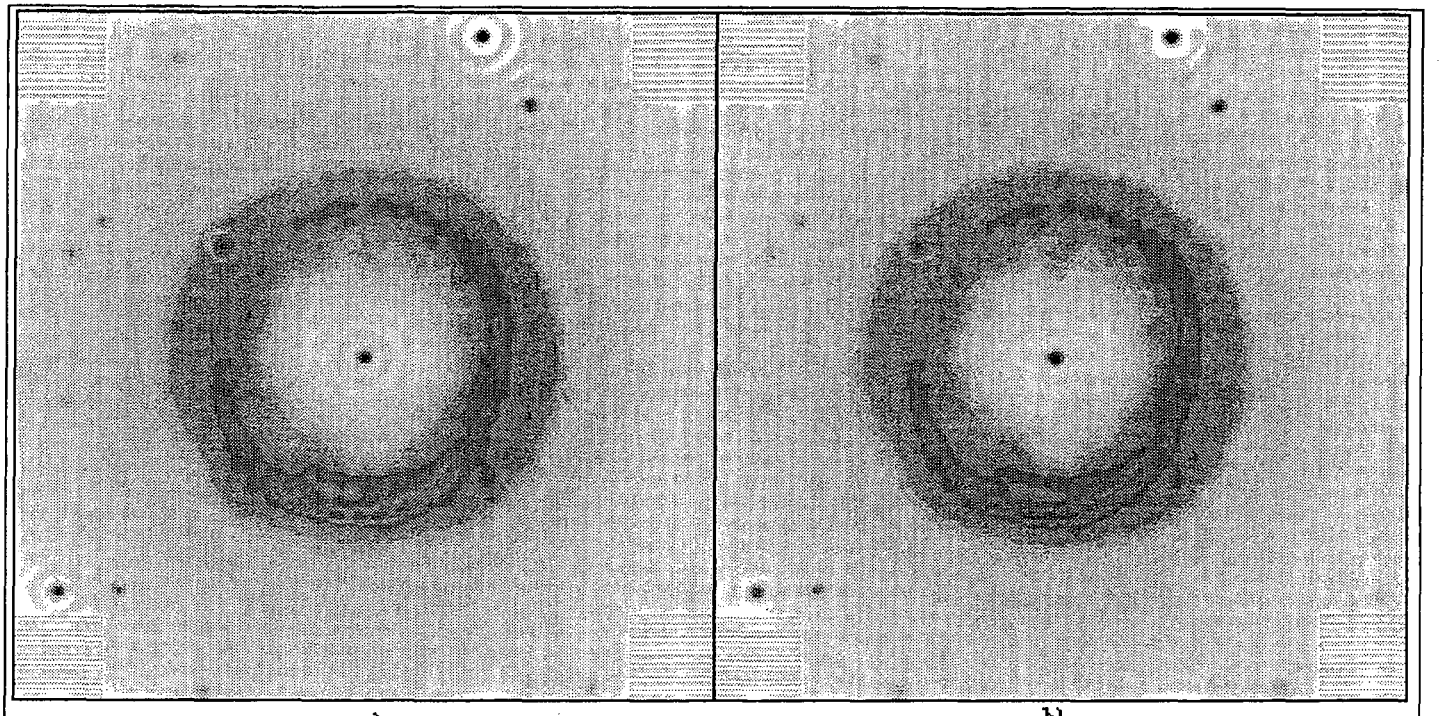

a) b)

Fig. 8 - Results of reconstructions of noise-free data, with sinusoidally spaced bars introduced in the initial image. a) Hubble simulation, 500 its. b) Reduced resolution simulation, 2000 its.

TABLE II

Energy included in 3 x 3 area and contrast in bar patterns, 7 x 7 area. Noise-free case.

Description	True data	Initial image	Hubble, 500 its.	Red. res, 2000 its.
Brightest star	51457		50416	48088
Central star	15125		13179	12060
Star included in nebula	5127		3626	3561
Low intensity star	1077		696	708
Bar pattern # 1, stadev.		18.22	1.73	1.59
# 2		17.18	1.09	1.08
# 3		18.44	1.31	1.36
# 4		17.42	1.70	1.78

of counts originally in the "pn" data generated at STSCI have been considered to be photons, without conversion factors. Fig. 9 shows the resulting simulated data. The reconstructions have been carried out by the standard MLE process, with stopping points at a number of selected iterations. Since we know that different parts of the image will become feasible at different iterations[7,8], no attempt has been made to apply a single cross-validation criterion as a stopping rule[9].

2.2.3.2 Analysis of reconstruction results

A method that appears to be in substantial use for examining results of reconstructions is to observe a map of residuals, i.e., the magnitude of the differences between the data and the projection of the reconstruction into data space. A variation of the above that ties with the concept of "weak feasibility"[10] is to modify that map to show the quotient

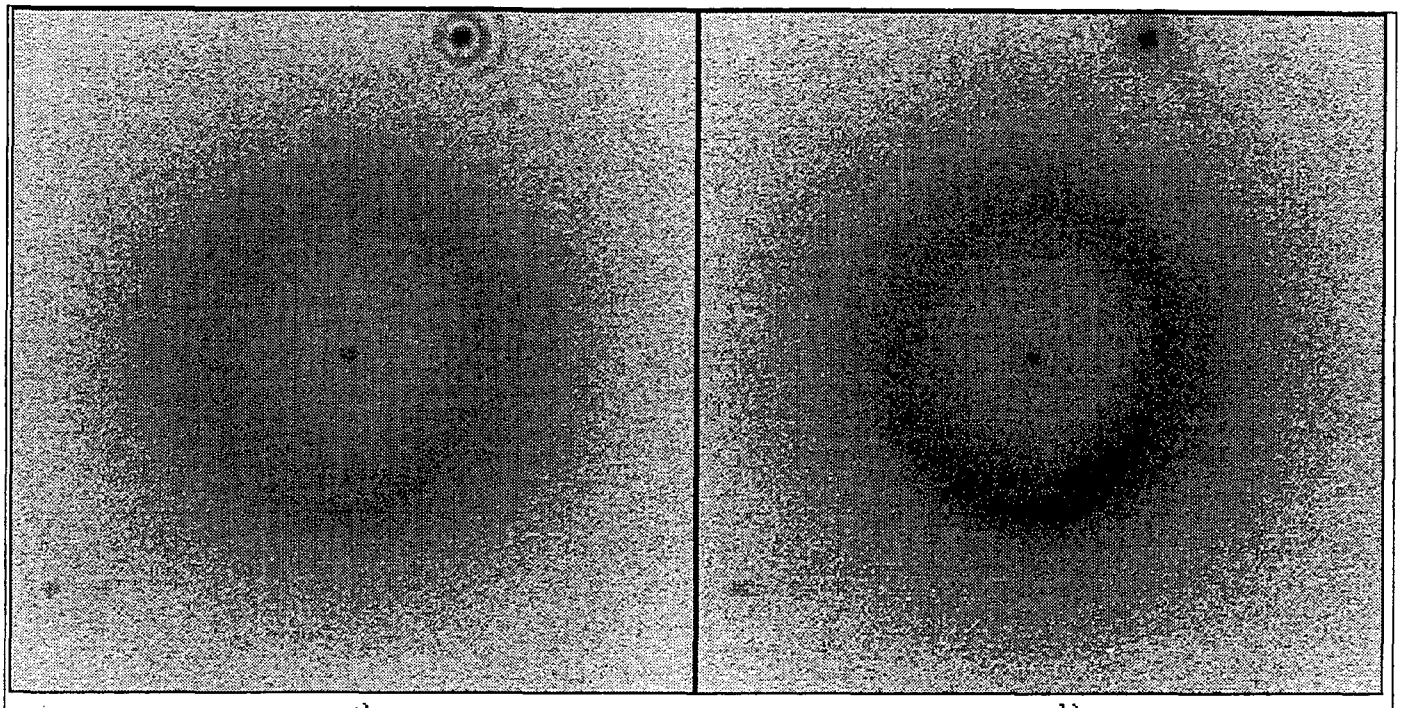

a) b)

Fig. 9 - Data used for the reconstructions with Poisson noise. Logarithmic gray scale. a) For Hubble simulation. b) For reduced resolution telescope.

$$r = \frac{\left(g_j - \sum_l h_{jl}\hat{f}_l\right)^2}{\sum_l h_{jl}\hat{f}_l} \tag{10}$$

which should average to 1.0 over locally homogeneous regions. Eq. 10 tests whether the values of the projection could be means of distributions that have the data as instances with the right variance for Poisson data. For the brighter stars in the "pn" phantom of Fig. 4 and Poisson data, this result is obtained approximately only at very high iteration numbers, when the energy enclosed in a 3 x 3 pixel array approaches the correct value (see Table I). For the weaker stars, the nebula and the "halo" around the nebula, values of r that average approximately 1.0 over a large number of relatively small homogeneous areas (up to 7 x 7 pixels) are obtained at a relatively low iteration number. It has been found that, both for the Hubble simulations and the reduced resolution telescope, the results at iterations 50 to 100 yield that average, coinciding with smooth reconstructions of the nebula and halo, but with poor resolution in the individual weaker stars. We shall now examine the obtained results at those iterations.

2.2.3.3 Resulting images

Figure 10a) shows the reconstruction results for the Hubble simulation with Poisson data at iteration 500, when the high intensity stars have been reconstructed with sharpness approaching that of the original phantom. The corresponding results for the reduced resolution telescope are shown in Fig. 10b), at 2000 iterations. It is evident that low intensity stars, the nebula and its halo are much worse in the second case than in the Hubble simulation.

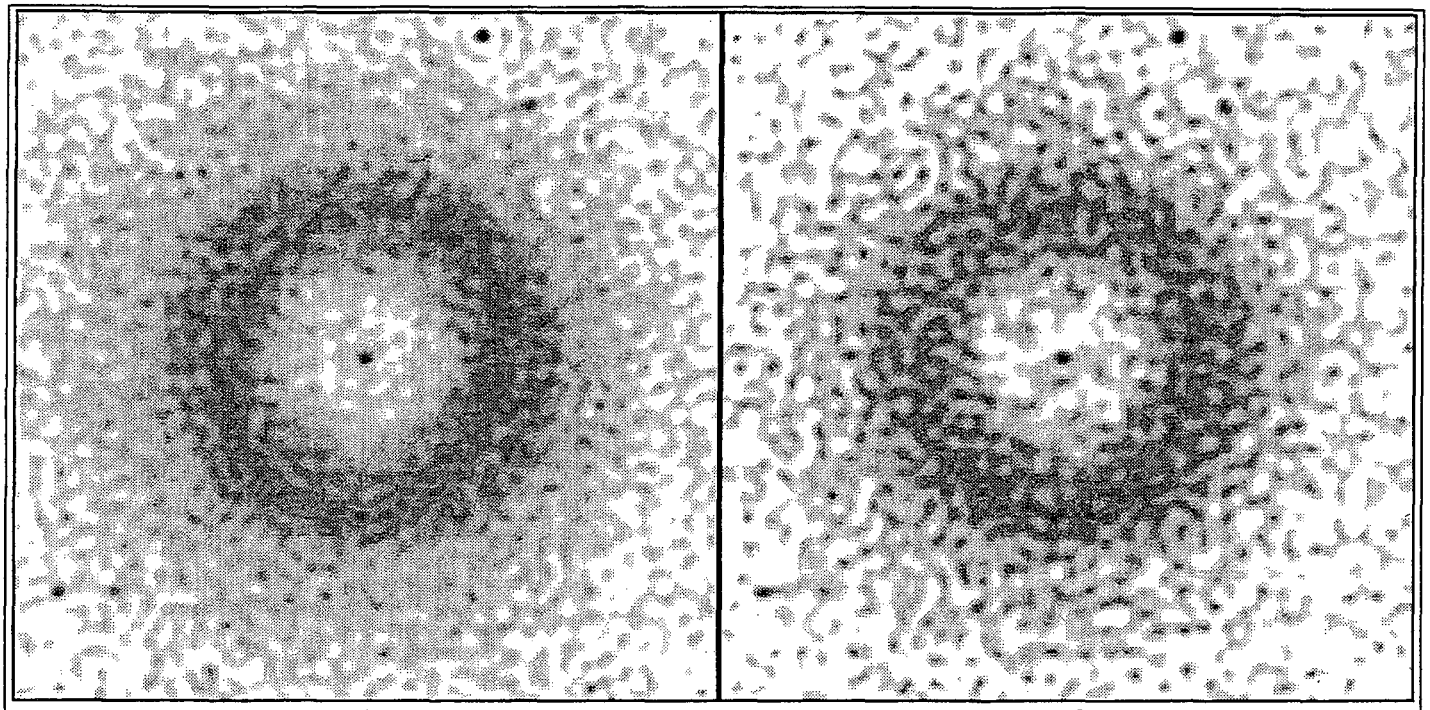

a) b)

Fig. 10 - Reconstructions of data with Poisson noise to a point with acceptable resolution in the brightest stars. a) Hubble simulation, 500 iterations. b) Reduced resolution simulation, 2000 iterations.

Figure 11a) shows the results for the Hubble simulation and Fig. 11b) those for the reduced resolution case, both at iteration 50, where the average value of r is approximately 1.0 for the nebula and the halo surrounding it. Both cases show smooth reconstructions of those structures, but the resolution for the stars in the second case is substantially worse than in the Hubble case.

The above results are consistent with what one would expect in a linear reconstruction method, i.e., a PSF that has many small values would be more sensitive to noise than a better PSF. It appears, then, that the MLE algorithm also behaves in the same reasonable way. The question arises as to whether the observed effects have anything to do with ghost images. Could one say, for example, that noise in the data "excites" the null component of the reduced resolution telescope and, for that reason, noise in the reconstruction is more prominent? The answer to this question is largely philosophical, but it appears that it is in the negative: reconstructions without noise, but with the introduction of ghost components, have shown that those components tend to vanish at large iteration numbers, while the noise magnification effects behave in the opposite way. The latter effects are well understood in terms of overfitting of the data and lead to the concept of feasibility, as discussed below.

3. WHAT DOES THE MLE ALGORITHM DO?

We recognize that the answer to this question is well known to many practicioners of image reconstruction, but we shall attempt to place it in the context of feasibility, which, we hope, may help in understanding some of the characteristics of MLE reconstructions. Simply stated, the MLE algorithm seeks to find the image $\hat{\mathbf{f}}$ whose projection into data space leads to the smallest residuals

$$g_j - \sum_l h_{jl} \hat{f}_l \,. \tag{11}$$

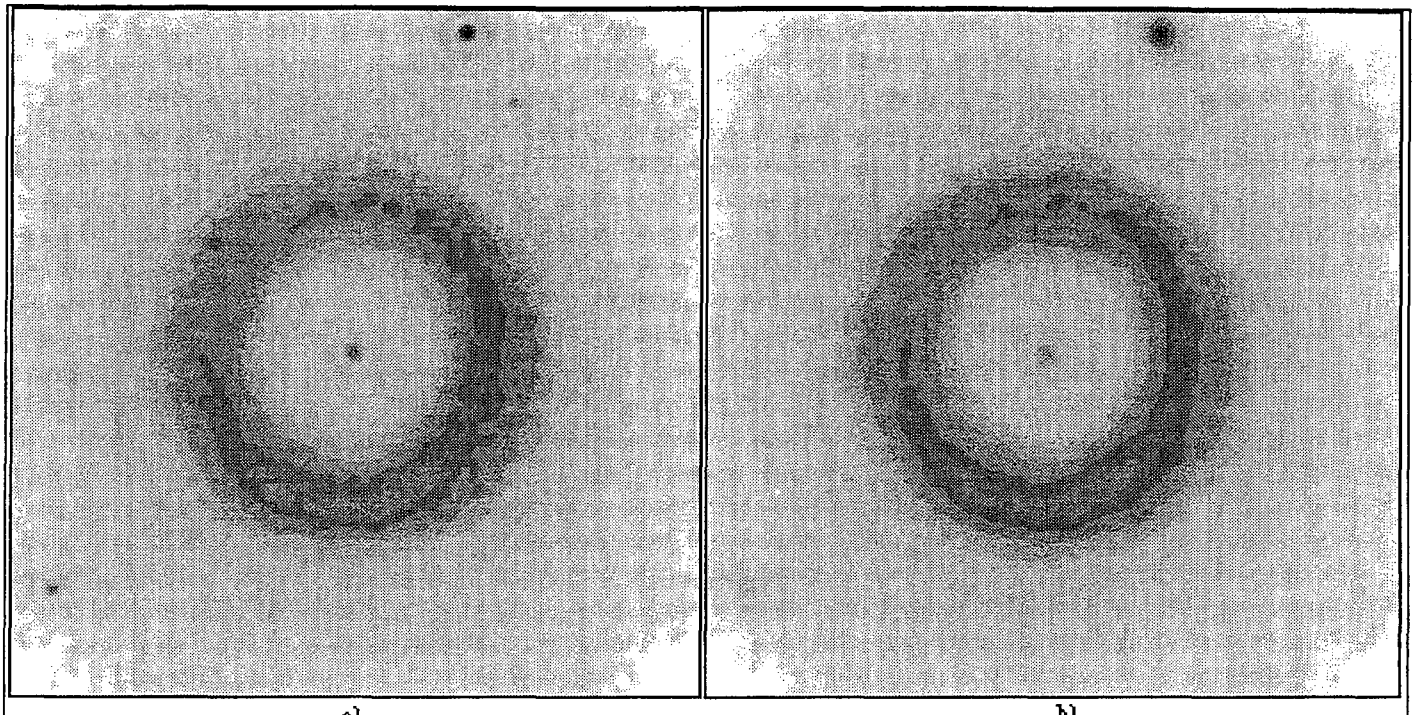

a) b)

Fig. 11 - Reconstructions of Poisson noise data at iteration 50, where residuals for the nebula and its surrounding halo indicated "weak feasibility" for those regions in the two cases: a) For Hubble simulation. b) For reduced resolution telescope.

This would not be particularly different from other methods of reconstruction, except that the measure of distance is taken in terms of the change of values of a Poisson distribution. The summation $\sum_l h_{jl}\hat{f}_l$ is considered to be the mean of a Poisson distribution of which g_j is a realization and the algorithm attempts to find the values $\hat{\mathbf{f}}$ that lead to smallest possible values of Eq. (11) by maximizing the global likelihood

$$L = \prod_j e^{-\sum_l h_{jl}\hat{f}_l} \frac{\left(\sum_l h_{jl}\hat{f}_l\right)^{g_j}}{g_j!} \quad . \tag{12}$$

Since the shape of the Poisson distribution and its variance depend on the number of counts, changing one count in a small $\hat{f}_l$, for example, will result in a larger change in the overall likelihood L than changing one count in a large $\hat{f}_l$. If we notice that Poisson distributions are at a maximum when the realization approaches the mean, we can see that the MLE tries to obtain the smallest residuals consistent with Eq. (12). At convergence, MLE images invariably appear very noisy because of that attempt to minimize the residuals, i.e., the data are overfitted. For that reason, we have proposed that a reconstruction should be stopped at some point when the image is locally "feasible", i.e., anytime that the image, if it were the true distribution of sources in the sky, could have given the measured data by a Poisson process (in the simplest imaging case)[11].

4. DISCUSSION AND CONCLUSION

In 2- or 3-dimensional medical tomography, it is easy to conceive and actually fabricate instruments that have null components. All that is needed is that the object to be imaged be not observed by a complete set of projections. In 2-dimensional reconstructions, that implies that some of the detectors on a plane are missing by necessity of the design or by damage during

operation. In 3-dimensional tomography, there will be null components because it is not economically feasible to surround a patient by a 4π solid angle of detectors. A number of techniques are in a more or less advanced stage of research to carry out reconstructions by linear (fast) methods of reconstruction. They usually require to infer the "missing cones" in frequency domain by some extrapolation of the available data. With the MLE method (slow) that extrapolation is unnecessary. The true PSF of the instrument is all that is necessary to solve the imaging problem, with results that do not exhibit catastrophic artifacts due to the omission of object views.

In the case of telescopes, it appears very unlikely that an instrument will be designed that will have missing values in the frequency domain. Even an instrument with a PSF showing strong shadows due to either a poor secondary or to mirror supports will have a complete set of values in frequency domain. Of course, an optical designer that wanted to build a telescope with exact zero components at some frequency could do it by properly masking the optics at the right places, but let's not consider such an extreme case. In particular, the uncorrected Hubble telescope does not have null images, whether reconstructions are carried out by linear or non-linear methods, since such images depend exclusively on the properties of the PSF. What we have attempted to show in this paper is that, if the uncorrected Hubble telescope were sampled at a finer resolution than the example shown in the paper, with a larger number of pixels than 512 x 512, so that the fall-off of the frequency response would be observable in the transform of the PSF, the MLE method of reconstruction still is well behaved with respect to the corresponding "nearly null images". We have done that by simulting a telescope with such a fall-off starting from the Hubble PSF. Clearly, it may not pay to attempt to use the enhanced resolution that higher sampling would give in the presence of noise. The reconstructions exhibit slower convergence rates and more sensitivity to noise due to the presence of the low values in the tails of the Fourier transform of the PSF. The MLE shows the typical trade-off between resolution and noise just as much as linear methods of reconstruction.

In conclusion, we can state that, from the point of view explored in this paper, the MLE or Richardson-Lucy algorithm is a robust method of reconstruction for astronomical images, particularly for the uncorrected Hubble telescope. The problems with the algorithm as one proceeds towards convergence are due to attempts at local overfitting of the data. This knowledge encourages us to continue in the path towards an automatic selection of local hyperparameters in a Bayesian method of reconstruction with entropy prior, following the work that we have recently published[12].

5. ACKNOWLEDGMENTS

The work of Jorge Llacer has been supported by the Director, Office of Energy Research, Office of Health and Environmental Research, Physical and Technological Division, of the U.S. Department of Energy under Contract No. DE-AC03-76SF00098. Jorge Nunez has been supported by, in part, by the DGICYT Ministerio de Educacion y Ciencia (Spain) under Grant No. BP90-0478 and fellowship No. BEC 91-328. Partial support for the collaborative work has been obtained from the Generalitat de Catalunya and the Gaspar de Portola Catalonian Studies Program of the University of California, Berkeley.

6. REFERENCES

1. H.H.Barrett, J.N. Aarsvold and T.J. Roney, "Null functions and eigenfunctions: tools for the analysis of imaging systems", in *Information Processing in Medical Imaging,* D.A. Ortentahl and J. Llacer, Eds., Wiley-Liss, pp. 211-226, 1991.

2. K.C. Andrews and B.R. Hunt, *Digital Image Restoration,* Prentice-Hall, Englewood Cliffs, 1977. Section 8.3.

3. L.A. Shepp and Y.Vardi, "Maximum likeliyood reconstruction for emission tomography", *IEEE Trans. Med. Imaging,* Vol. MI-1, pp. 113-121, June 1982.

4. W.H.Richardson, "Bayesian-Based Iterative Method of Image Restoration", *J. Opt. Soc. Am.*, Vol. 62, No. 1, pp. 55-59, Jan. 1972.

5. B. Lucy, "An iterative technique for the rectification of observed distributions", *The Astronomical Journal,* Vol. 79, No. 6, pp. 745-754, June 1974.

6. W.H. Press, et al, *Numerical Recipes in C,* Cambridge Univ. Press, 1990.

7. R.L. White, "Image restoration using the Richardson-Lucy method", in *The restoration of HST Images and Spectra II,* Proc. Workshop held at the Space Telescope Science Institute, R.J. Hanisch and R.L. White, Eds., Baltimore, Nov. 1993, in press.

8. J. Nunez and J. Llacer, "HST image reconstruction with variable resolution", in *The restoration of HST Images and Spectra II,* Proc. Workshop held at the Space Telescope Science Institute, R.J. Hanisch and R.L. White, Eds., Baltimore, Nov. 1993, in press.

9. K.J. Coakley and J. Llacer, "The use of cross-validation as a stopping rule in emission tomography image reconstruction", *Proc. SPIE Conf. on Medical Imaging V:, Image Physics,* Vol. 1443, pp. 226-233, Feb. 1991.

10. J. Llacer and E. Veklerov, "Feasible images and practical stopping rules for iterative algorithms in emission tomography", *IEEE Trans. Med. Imaging,* Vol. 8, No. 2, pp. 186-319, June 1989.

11. J. Llacer and J. Nunez, "Iterative maximum likelihood estimator and Bayesian algorithms for image reconstruction in astronomy", in *The restoration of HST images and spectra,* Proc. Workshop, STSCI, R.L. White and R.J. Allen, Eds., 1990.

12. J. Nunez and J. Llacer, "A general Bayesian image reconstruction algorithm with entropy prior. Preliminary application to HST data", *Pub. of Astr. Soc. Pacific,* Vol. 105, pp. 1192-1208, October 1993.

LAWRENCE BERKELEY LABORATORY
UNIVERSITY OF CALIFORNIA
TECHNICAL INFORMATION DEPARTMENT
BERKELEY, CALIFORNIA 94720